Journal of Hydrology 522 (2015) 58–66

Contents lists available at ScienceDirect

Journal of Hydrology

journal homepage: www.elsevier.com/locate/jhydrol

Spatial patterns of throughfall isotopic composition at the event and seasonal timescales

Scott T. Allen [a,*], Richard F. Keim [a], Jeffrey J. McDonnell [b,c,d]

[a] School of Renewable Natural Resources, Louisiana State University, Baton Rouge, LA, USA
[b] Global Institute for Water Security, University of Saskatchewan, Saskatoon, Canada
[c] School of Geosciences, University of Aberdeen, Aberdeen, Scotland, UK
[d] Dept of Forest Engineering, Resources and Management, Oregon State University, Corvallis, OR, USA

ARTICLE INFO

Article history:
Received 22 May 2014
Received in revised form 20 October 2014
Accepted 13 December 2014
Available online 20 December 2014
This manuscript was handled by Laurent Charlet, Editor-in-Chief, with the assistance of Fereidoun Rezanezhad, Associate Editor

Keywords:
Stable isotopes
Spatiotemporal variability
Sampling error
Net precipitation
Canopy interception

SUMMARY

Spatial variability of throughfall isotopic composition in forests is indicative of complex processes occurring in the canopy and remains insufficiently understood to properly characterize precipitation inputs to the catchment water balance. Here we investigate variability of throughfall isotopic composition with the objectives: (1) to quantify the spatial variability in event-scale samples, (2) to determine if there are persistent controls over the variability and how these affect variability of seasonally accumulated throughfall, and (3) to analyze the distribution of measured throughfall isotopic composition associated with varying sampling regimes. We measured throughfall over two, three-month periods in western Oregon, USA under a Douglas-fir canopy. The mean spatial range of $\delta^{18}O$ for each event was 1.6‰ and 1.2‰ through Fall 2009 (11 events) and Spring 2010 (7 events), respectively. However, the spatial pattern of isotopic composition was not temporally stable causing season-total throughfall to be less variable than event throughfall (1.0‰; range of cumulative $\delta^{18}O$ for Fall 2009). Isotopic composition was not spatially autocorrelated and not explained by location relative to tree stems. Sampling error analysis for both field measurements and Monte-Carlo simulated datasets representing different sampling schemes revealed the standard deviation of differences from the true mean as high as 0.45‰ ($\delta^{18}O$) and 1.29‰ (d-excess). The magnitude of this isotopic variation suggests that small sample sizes are a source of substantial experimental error.

1. Introduction

Stable isotopes of water are useful for tracing the movement of water through catchments (Kendall and McDonnell, 1998). The isotopic composition of precipitation and other end members are used as input signals for estimating streamwater sources (Klaus and McDonnell, 2013), transit time (Tetzlaff et al., 2011), plant water sources (Goldsmith et al., 2012), and multiple other applications.

However, precipitation rarely infiltrates or runs off without some preceding fractionating process (Gat and Tzur, 1968). Rainfall from the open sky (gross precipitation; P_g) is intercepted by vegetation canopies resulting in some evaporation (interception loss). The remainder reaches the soil as throughfall (TF), composed of both water that bypasses or is temporarily intercepted by the canopy, or as stemflow that runs down the bark surfaces. Consequently, interception changes numerous characteristics of precipitation (Levia et al., 2011), including its isotopic composition. Throughfall is generally heavier isotopically than P_g, but variable within and among events (Ikawa et al., 2011; Kato et al., 2013; Saxena, 1986). Kubota and Tsuboyama (2003) showed that ignoring the isotopic difference between TF and P_g is a source of error in storm hydrograph separation. Accordingly, TF isotopic composition is a more appropriate input concentration for models that employ stable isotopes of precipitation for water tracing.

Event-mean isotopic differences between TF and P_g have been the focus of previous studies (e.g., Ikawa et al., 2011; Saxena, 1986), but few studies to date have examined the spatial variability of throughfall isotopic composition within and among events. Recent work has shown that, within short measurement periods, the range in isotopic composition at individual TF sampling locations can exceed the difference between open precipitation and TF (Allen et al., 2014; Brodersen et al., 2000; Kato et al., 2013).

* Corresponding author at: School of Renewable Natural Resources, Louisiana State University, 227 Renewable Natural Resources Bldg., Baton Rouge, LA 70803, USA. Tel.: +1 225 578 0996.
E-mail address: salle48@lsu.edu (S.T. Allen).

http://dx.doi.org/10.1016/j.jhydrol.2014.12.029
0022-1694/

This intra-event spatial variability is substantial and may parallel the well-known spatial variability observed for TF amount (Raat et al., 2002).

At the plot scale, TF amount is often autocorrelated spatially (Gerrits et al., 2010; Keim et al., 2005; Loescher et al., 2002) and temporally (Gerrits et al., 2010; Keim et al., 2005; Raat et al., 2002; Staelens et al., 2006). This has been largely attributed to canopy architecture (Gerrits et al., 2010; Staelens et al., 2006; Whelan and Anderson, 1996). Studies of the spatial structure of TF amount have led to improved sampling as well as realization of how TF variability affects subsurface hydrology (Coenders-Gerrits et al., 2013; Hopp and McDonnell, 2011; Raat et al., 2002). Because spatial patterns in TF amount are temporally persistent, repeated sampling in fixed or too few locations can result in large anomalies in estimates of the mean. Thus randomly relocating TF collectors between events (roving collectors) has been advocated as a way to reduce measurement uncertainty (Holwerda et al., 2006; Ritter and Regalado, 2014).

Multiple interacting processes affect TF. Consequently the relationship between amount and isotopic composition is complex (Brodersen et al., 2000; Saxena, 1986). One important process controlling isotopic composition appears to be time-varying transmission of precipitation (that varies in isotopic composition through the event) through the canopy (i.e., the 'selection' process; Brodersen et al., 2000; DeWalle and Swistock, 1994; Ikawa et al., 2011; Kato et al., 2013). Evaporative fractionation (Kato et al., 2013) and isotopic exchange (Kendall, 1993; Saxena, 1986) can occur and result in complex relations with spatial variability in TF amount. Understanding this spatiotemporal variability of TF isotopic composition is critical for using TF as an input value or end member in isotope tracer studies. Understanding such behavior also offers potential mechanistic insights into intra-canopy processes during rainfall (Allen et al., 2014).

While the spatiotemporal variability of TF amount has been addressed and has led to comprehensive analyses of sampling errors in TF amount (Ritter and Regalado, 2010; Zimmermann et al., 2010), strategies to sample throughfall for isotopic composition are poorly developed. Such study requires consideration of a suite of controlling processes that likely differ from those controlling TF amount.

Here we characterize the spatiotemporal structure of coupled amount and isotopic composition variability of throughfall. Specifically, we measured throughfall amount and isotopic composition over two three-month periods to address three objectives: (1) to quantify the spatial variability of isotopic composition at the event scale, (2) to determine if there are persistent controls over the variability and how these affect variability of seasonally accumulated throughfall, and (3) to analyze the distribution of measured TF isotopic composition associated with varying number of collectors and using fixed versus roving collectors.

2. Methods

2.1. Site description

This study was conducted in Watershed 1 (WS1) of the H.J. Andrews Experimental Forest in the western Cascade Range of Oregon, which has been extensively described in previous studies (e.g., Lutz and Halpern, 2006; Rothacher, 1965). The steeply-sloped, 96 ha basin was clear-cut harvested in the late 1960s and is now covered with a dense canopy dominated by Douglas-fir (*Pseudotsuga menziesii*). The climate is typical of the Pacific Northwest; mean annual precipitation exceeds 2000 mm with 80% falling between October and April. All TF collection was at plots at 500 m elevation. Humidity and rainfall intensity were measured at the H.J. Andrews benchmark meteorological station about 500 m from the study plots.

Two separate experiments were conducted. Experiment 1 (Exp1) took place on a relatively flat area of predominantly Douglas-fir forest coinciding with a 75 m long section of a study transect established in 1962 (Halpern and Dyrness, 2010) and the site of multiple ecological and hydrological experiments (e.g., Bond et al., 2002; Halpern and Franklin, 1990). Experiment 2 (Exp2) used a pair of 12 × 5 m plots as a north-aspect-plot (NAP) and a south-aspect-plot (SAP), 100 m apart on steep opposite slopes of WS1. Canopy cover for SAP and NAP was 92% and 95% respectively, estimated using Fusion software (United States Forest Service Remote Sensing Applications Center, Salt Lake City, UT) from a LiDAR flight in August, 2008. Canopy cover for Exp1 was not quantified but was similar to Exp2. Three P_g collectors were located within 180 m of all sampling plots in a 0.04 ha clearing surrounded by trees 15–20 m tall.

2.2. Sample collection

Experiment 1, described by Allen et al. (2014), was conducted between October and December 2009. Sampling was by 13 TF collectors with 9.5 cm diameter openings placed along the transect under Douglas-fir trees, randomly with respect to boles, crowns, and other collectors. Storms were sampled per event and collected after precipitation and the majority of drip ceased. Logistical constraints caused some sampling periods to consist of multiple consecutive storm events, yielding 11 collection periods (1.1–1.11). Intra-event dry periods never exceeded 2 days.

Experiment 2 was conducted between April and July 2011 and used higher spatial density of collectors than Exp1 to better characterize spatial patterns. Thirty-six collection points were established at random positions in each plot. Eighteen TF collectors were used at each 12 × 5 m plot and were randomly relocated among the 36 fixed locations for each sampling period. Inter-collector distances ranged from 0.2 m to 12 m with a mean distance of 4.3 m. Both P_g and TF were collected with 2 l polyethylene bottles attached to 15.5 cm diameter funnels about once per week, depending on precipitation. Within the sampling periods, there was never more than one calendar day without rain. There was a total of seven Exp2 collection periods (2.1–2.7; Table 1).

For sampling during both experiments, the volume of water accumulated in each collector was measured and a zero headspace subsample was taken with a 20 ml glass vial for isotope analysis.

2.3. Analyses

We calculated interception loss as the difference between mean P_g and TF for each event, and a volume weighted mean over all events for seasonal interception loss. Although stemflow occurs, we assumed it was not substantial in Douglas-fir forest (Link et al., 2004; Rothacher, 1963).

All isotope data are expressed in terms of δ, calculated as:

$$\delta = \left(\frac{R_{\text{sample}}}{R_{\text{V-SMOW}}} - 1\right) \times 1000‰ \quad (1)$$

where V-SMOW is the Vienna Standard Mean Ocean Water (Coplen et al., 2002) and R is $^{18}O/^{16}O$ or $^{2}H/^{1}H$. Water samples from Exp1 were analyzed for δ^2H and $\delta^{18}O$ on an off-axis integrated cavity output laser spectrometer (Los Gatos Research LWIA, Mountain View, CA) by the Institute for Water and Watersheds Collaboratory (Corvallis, Oregon). Accuracy was 0.18 ± 0.07‰ and −1.02 ± 0.92‰ (mean ± standard error) for $\delta^{18}O$ and δ^2H respectively, calculated as deviation of a third standard from a two-point calibration line

Table 1
Amount, intensity, and isotopic composition of throughfall and gross precipitation for events during the Experiments 1 and 2 collection periods (mean ± standard deviation). The difference of throughfall from gross precipitation is indicated by Δ. The precipitation events contributing to Exp2 NAP are the same as for the SAP so these values are not repeated in the table.

Exp1 events	Date	Gross precipitation (P_g)				Throughfall (TF)			TF − P_g		
		Amount (mm)	Intensity (mm/h)	$\delta^{18}O$ (‰)	d-excess (‰)	Amount (mm)	$\delta^{18}O$ (‰)	d-excess (‰)	Loss (%)	$\Delta\delta^{18}O$ (‰)	Δd-excess (‰)
1.1	9 Oct–10 Oct	40	1.7	−6.7	11.7	30 ± 6	−6.7 ± 0.3	11.0 ± 0.4	23.8	−0.0	−0.7
1.2	22 Oct–23 Oct	14	0.8	−9.7	10.3	10 ± 3	−8.5 ± 0.4	11.1 ± 0.6	27.6	1.3	0.8
1.3	23 Oct–24 Oct	62	2.9	−14.2	13.0	52 ± 9	−13.9 ± 0.4	11.2 ± 0.8	16.3	0.4	−1.8
1.4	24 Oct–27 Oct	82	1.7	−8.8	21.7	68 ± 22	−8.4 ± 0.4	20.5 ± 1.0	17.5	0.4	−1.2
1.5	27 Oct–2 Nov	43	0.8	−10.1	8.4	40 ± 27	−9.3 ± 0.9	10.0 ± 0.7	6.3	0.8	1.6
1.6	2 Nov–8 Nov	52	1.5	−15.4	9.6	43 ± 9	−15.0 ± 0.4	8.4 ± 2.2	17.4	0.4	−1.2
1.7	8 Nov–10 Nov	49	1.5	−10.9	16.7	46 ± 27	−10.5 ± 0.5	16.4 ± 2.5	5.0	0.5	−0.3
1.8	10 Nov–16 Nov	32	0.6	−6.2	11.8	30 ± 8	−6.2 ± 0.2	11.8 ± 1.1	4.6	0.1	−0.0
1.9	16 Nov–19 Nov	45	2.0	−10.9	12.7	42 ± 21	−10.3 ± 0.3	12.8 ± 0.6	6.7	0.7	0.1
1.10	6 Dec–8 Dec	11	1.1	−9.9	15.0	9 ± 3	−11.0 ± 0.4	15.4 ± 1.2	20.9	−1.1	0.4
1.11	8 Dec–10 Dec	49	1.7	−7.5	18.7	4 ± 27	−7.2 ± 0.3	17.1 ± 1.5	9.3	0.3	−1.7
Exp2 events, South Aspect Plot											
2.1	2 April–9 April	83	1.4	−9.7	11.0	58 ± 18	−9.0 ± 0.3	10.2 ± 1.2	30.1	0.7	−0.8
2.2	10 April–16 April	91	1.1	−12.7	10.4	63 ± 17	−12.6 ± 0.3	10.9 ± 0.6	30.8	0.1	0.5
2.3	20 April–26 April	65	0.9	−8.0	8.5	37 ± 11	−7.3 ± 0.2	8.5 ± 0.8	42.3	0.7	0.1
2.4	2 May–12 May	35	0.7	−9.6	6.4	19 ± 6	−9.3 ± 0.2	5.2 ± 0.7	47.0	0.3	−1.2
2.5	15 May–22 May	25	0.8	−8.1	11.4	14 ± 4	−6.1 ± 0.3	9.4 ± 1.0	44.8	2.0	−1.9
2.6	22 May–27 May	69	1.3	−10.0	8.9	45 ± 14	−9.8 ± 0.2	8.4 ± 0.6	35.9	0.2	−0.5
2.7	28 June–1 July	15	1.0	−8.0	4.5	9 ± 4	−7.2 ± 0.2	2.6 ± 0.8	38.3	0.8	−1.9
Exp2 events, North Aspect Plot											
2.1	2 April–9 April					68 ± 14	−8.9 ± 0.2	10.8 ± 0.9	18.1	0.8	−0.1
2.2	10 April–16 April					72 ± 12	−12.6 ± 0.2	10.5 ± 0.5	20.4	0.1	0.1
2.3	20 April–26 April					48 ± 9	−7.4 ± 0.2	8.9 ± 0.7	25.2	0.6	0.5
2.4	2 May–12 May					21 ± 4	−9.3 ± 0.1	5.6 ± 0.7	38.6	0.3	−0.8
2.5	15 May–22 May					15 ± 4	−6.5 ± 0.4	9.0 ± 1.4	39.8	1.6	−2.3
2.6	22 May–27 May					49 ± 13	−9.8 ± 0.3	8.5 ± 1.1	29.0	0.2	−0.4
2.7	28 June–1 July					11 ± 2	−7.2 ± 0.3	2.2 ± 1.0	28.2	0.7	−2.3

(IAEA, 2009). All three standards were used in the data calibration to improve upon the reported accuracy. Precision, quantified as the pooled standard deviation of three repeated measurements of every sample, was 0.07‰ and 0.28‰ for $\delta^{18}O$ and $\delta^{2}H$ respectively. Samples from Exp2 were analyzed on a cavity ringdown laser spectrometer (Picarro L-1102, Santa Clara, CA). The accuracy of our analyses was −0.28 ± 0.09‰ and −0.68 ± 0.77‰ for $\delta^{18}O$ and $\delta^{2}H$ respectively, calculated using the same protocol as for Exp1. The precision between repeated measures was 0.12‰ and 0.57‰ for $\delta^{18}O$ and $\delta^{2}H$ respectively.

We used d-excess to indicate deviation from the meteoric water line (MWL) and likely non-equilibrium fractionation by evaporation (Gat, 1996):

$$\text{d-excess} = \delta^{2}H - 8 \times (\delta^{18}O) \quad (2)$$

In this paper, we use the symbol Δ to indicate the TF − P_g difference:

$$\Delta\delta^{18}O = \delta^{18}O_{TF} - \delta^{18}O_{P_g} \quad (3)$$

$$\Delta\text{d-excess} = \text{d-excess}_{TF} - \text{d-excess}_{P_g} \quad (4)$$

All statistical analyses were run on MATLAB (MathWorks, Natick, MA).

2.3.1. Temporal persistence

Temporal persistence was analyzed by standardizing collector amount and isotopic composition for each event by subtracting the event mean and dividing by the event standard deviation (i.e., z scores). Temporal persistence is indicated by consistently positive or negative standardized values at each location and less scatter at a collector indicates more stable relative amount (or $\delta^{18}O$, or d-excess) at that point (Keim et al., 2005; Vachaud et al., 1985). This analysis does not account for the spatial arrangement, but time stability suggests fixed spatial controls (Staelens et al., 2006). Kruskal–Wallis (KW) tests were used to test hypotheses of the general effect of location on throughfall amount and isotopic composition.

2.3.2. Throughfall sampling simulation

We estimated the sampling error distributions for TF amount, $\delta^{18}O$, and d-excess using Monte-Carlo simulations to answer the question of how sampling error is dependent on sampling strategy (e.g., Ritter and Regalado, 2014). Specific comparisons were errors associated with individual events versus cumulative sampling (Exp1 and Exp2), roving versus fixed location collectors for cumulative sampling (Exp1 only; Exp2 dataset used roving collectors so we could not simulate fixed sampling), and for single versus multiple (maximum 10) collectors (Exp1 and Exp2).

In each iteration of Monte Carlo simulations, a subset of collectors (N = 1,2,..., 10) was selected at random and weighted mean sample amount, $\delta^{18}O$, and d-excess were calculated and compared to the respective population means; this was iterated 10,000×, sufficient for reaching asymptotic behavior. For Exp2, measurements were transformed as deviations from plot means (NAP or SAP) rather than whole population mean. For cumulative sampling, the set of N collectors used across all events of each season was either fixed (fixed cumulative TF), or randomly reselected by event (roving cumulative TF). Although similar analyses have been used in TF amount studies with up to hundreds of collectors (Ritter and Regalado, 2014; Zimmermann et al., 2010), we limited simulations to maximum 10 collectors to simulate the sample sizes more common to isotope studies.

2.3.3. Variograms

Variograms were used to assess the spatial dependence of TF amount, $\delta^{18}O$, and d-excess. Experimental variograms (Keim et al., 2005) were created with the variance, γ_h, defined as:

$$\gamma_h = \sum \frac{(z_x - z_{x+h})^2}{n} \quad (5)$$

where z_x is the parameter of interest (amount, d-excess, or $\delta^{18}O$) at point x, z_{x+h} is the value at another point separated by lag h, and n is the number of pairs. The maximum lag distance calculated was half of the longest lag to avoid edge effects. Variance was calculated for 20 bins of equal n.

3. Results

3.1. Overview

Precipitation differed between Exp1 and Exp2. Events in Exp1 were longer duration and higher amount than more frequent and smaller events in Exp2. In Exp1, rain occurred 75% of days (mean 11.2 mm/day), and in Exp2, rain occurred 71% of days (mean 6.3 mm/day). Some events were missed because of logistical constraints so not all events are consecutive. Measured P_g was 477 mm and 382 mm for Exp1 and Exp2, respectively (Table 1).

Interception loss was greater during Exp2, with 36% for the SAP and 26% for the NAP versus 14% loss in Exp1. For Exp1, event-mean interception loss was not strongly related to event size ($r^2 = 0.07$, $p = 0.45$) or precipitation intensity ($r^2 < 0.01$, $p = 0.87$). For Exp2, event-mean interception loss was negatively related to event size ($r^2 = 0.60$, $p = 0.04$) and precipitation intensity ($r^2 = 0.71$, $p = 0.02$). For Exp1 and Exp2 (respectively) over all sampling periods, the mean minimum TF amounts measured at any single collector were 39% and 31% of P_g and mean maximum amounts measured were 179% and 96% of P_g, demonstrating a large range among collectors.

In Exp1, $\Delta\delta^{18}O$ (difference of P_g from TF) was generally positive (0.3 ± 0.7‰; mean ± SD), that is TF $\delta^{18}O$ was generally heavier than P_g; the mean range of spatial variation was 1.6 ± 0.8‰. In Exp2, TF $\Delta\delta^{18}O$ was positive for every sampling period (0.7 ± 0.6‰) and the range of spatial variation was 1.2 ± 0.4‰. Event means for Exp2 $\Delta\delta^{18}O$ ranged from 0.2‰ to 1.8‰ (Table 1). In both Exp1 and Exp2, $\Delta\delta^{18}O$ was not strongly correlated with event size ($r^2 = 0.05$, $p = 0.52$ and $r^2 = 0.30$, $p = 0.21$ for Exp1 and Exp2, respectively), event-mean percent interception loss ($r^2 = 0.01$, $p = 0.78$; $r^2 = 0.18$, $p = 0.34$), or precipitation intensity ($r^2 < 0.01$, $p > 0.99$; $r^2 = 0.10$, $p = 0.50$). Among events in both Exp1 and Exp2, event-mean absolute value of $\Delta\delta^{18}O$ was negatively correlated with event amount ($r^2 = 0.25$, $b = -0.01$‰ mm^{-1}, $p = 0.03$), so there was a slightly greater deviation of TF $\delta^{18}O$ from P_g with small events.

For Exp1 and Exp2, TF Δd-excess was not consistently positive or negative among events (Table 1) and varied significantly among collectors within events (Fig. 1). For Exp1, Δd-excess was negatively correlated with event size ($r^2 = 0.38$, $p = 0.04$) whereas Δd-excess was positively correlated with event size in Exp2 ($r^2 = 0.80$, $p < 0.01$). For both Exp1 and Exp2, Δd-excess was not correlated with event-mean percent interception loss ($r^2 = 0.01$, $p = 0.8$; $r^2 = 0.33$, $p = 0.18$). While Δd-excess was positively correlated with precipitation intensity in Exp1 ($r^2 = 0.67$, $p < 0.01$), it was not for Exp2 ($r^2 = 0.13$, $p = 0.42$). For Exp1, Δd-excess was −0.4 ± 1.1‰ (mean ± SD) with range among collectors of 5.0 ± 3.4‰ (mean ± SD). For Exp2, mean Δd-excess was −0.9 ± 0.9‰ ranging from −2.1‰ (events 2.5 and 2.7) to 0.3‰ (2.3). The range of d-excess among collectors by event was 3.9 ± 1.2‰.

Coinciding with the higher Exp2 interception loss, mean Exp2 TF $\Delta\delta^{18}O$ tended to be greater (0.67 ± 0.02‰; mean ± pooled SE), than Exp1 $\Delta\delta^{18}O$ (0.32 ± 0.02‰) and the Δd-excess during Exp2 (−0.80 ± 0.06‰; mean ± pooled SE) was more negative than the Δd-excess for Exp1 (−0.36 ± 0.13‰; mean ± pooled SE).

Despite the SAP having an average of 10.0% (of P_g) more interception loss than observed at the NAP, the two plots had generally similar mean values of $\delta^{18}O$ and d-excess (Table 1). *T*-tests showed

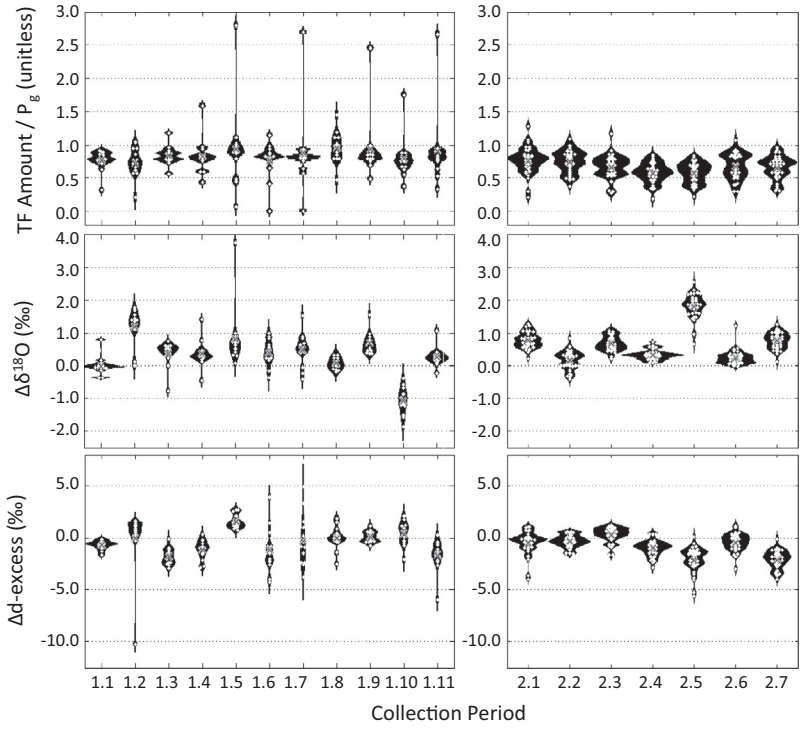

Fig. 1. Distribution plots of throughfall (TF) deviation from gross precipitation (P_g) for: amount (TF/P_g), $\Delta\delta^{18}O$ (Δ = TF − P_g), and Δd-excess. White dots are individual observations, in black are kernel-smoothed histograms, and gray 'X's are means.

no significant differences ($p > 0.05$) between NAP and SAP d-excess for any event.

3.2. Spatial heterogeneity and pattern stability

Spatial variability of TF varied by event and between Exp1 and Exp2. For Exp1, the shapes of the distributions and ranges in TF amount, $\Delta\delta^{18}O$, and Δd-excess varied among events (Fig. 1). During Exp2, both the shapes and ranges of distributions of TF amount were more similar among events (Fig. 1). Although the means varied, the ranges of $\Delta\delta^{18}O$ and Δd-excess were also fairly consistent among events during Exp2 (Fig. 1). Range of variation in $\delta^{18}O$ and d-excess were unrelated to TF amount or intensity for both Exp1 and Exp2 (all R^2 values ranged between 0.00 and 0.13).

For both Exp1 and Exp2, the spatial patterns in TF amount were temporally stable (Fig. 2). For Exp1, certain collectors tended to have consistently higher or lower amounts than others, however the range of variation for most collectors overlapped substantially (i.e., the trend from lowest to highest amount was mostly flat other than the tails). We interpret this as patch stability because there were a few locations distinct from the rest. In contrast, there was a steeper trend across the collectors in Exp2 which indicated a more continuous spectrum of variation (general stability). There was a weaker pattern in the NAP due to a wider range of variation at each collector. For Exp2, caution must be used in interpreting time-stability plots because each location had a different combination of contributing events.

For Exp1 and Exp2 (at both the NAP and SAP), there was a statistically significant collector effect among rank-transformed values (Kruskal–Wallis test, $p < 0.0001$). For Exp2, TF amount at the SAP was more temporally stable than at the NAP as indicated by tighter distribution around the mean (Fig. 2). For $\delta^{18}O$ and d-excess, there was no collector effect for Exp1 or Exp2 on either plot (Kruskal–Wallis test, $p > 0.1$).

3.3. Cumulative TF

The range of cumulative TF among collectors was lower than the range over all individual events, and the reduction in range was greater for $\delta^{18}O$ and d-excess (Fig. 3) than amount. The large range in cumulative TF amount was caused by temporal stability, so that cumulative amount range was only 10% lower than the mean range for individual events. In contrast, the range of cumulative $\Delta\delta^{18}O$ was 36% lower than the mean range of individual events; the range of cumulative Δd-excess was 62% lower than the mean range of individual events. The reduction in range from individual events to cumulative totals in isotopic composition indicates unstable spatial patterns that smoothed variability over time.

3.4. Simulated throughfall sampling variability

The TF sampling simulation showed that standard deviations of simulated, cumulative TF amount were less using roving rather than fixed-position samplers (Fig. 4A). Standard deviations for cumulative amount sampling at fixed locations were not substantially less than that of individual events.

In contrast, for isotopic composition, standard deviations were greater (d-excess) or similar ($\delta^{18}O$) with roving compared to fixed position samplers (Fig. 4B and C). For single collectors, the standard deviation around the true mean $\delta^{18}O$ exceeded 0.45‰ for individual events (Exp1) and was as high as 0.29‰ for cumulative $\delta^{18}O$. Use of either roving or fixed-position collectors reduced the $\delta^{18}O$ standard deviation as compared to individual events. The reduction in standard deviation with each added collector was greater for individual events than for cumulative. Standard deviations of amount, $\delta^{18}O$, and d-excess were greater for Exp1 than Exp2.

3.5. Spatial controls over patterns of heterogeneity (Experiment 2 only)

For Exp2, the distance to the nearest tree for each collector was inconsistently and weakly related to TF amount, $\delta^{18}O$, and d-excess

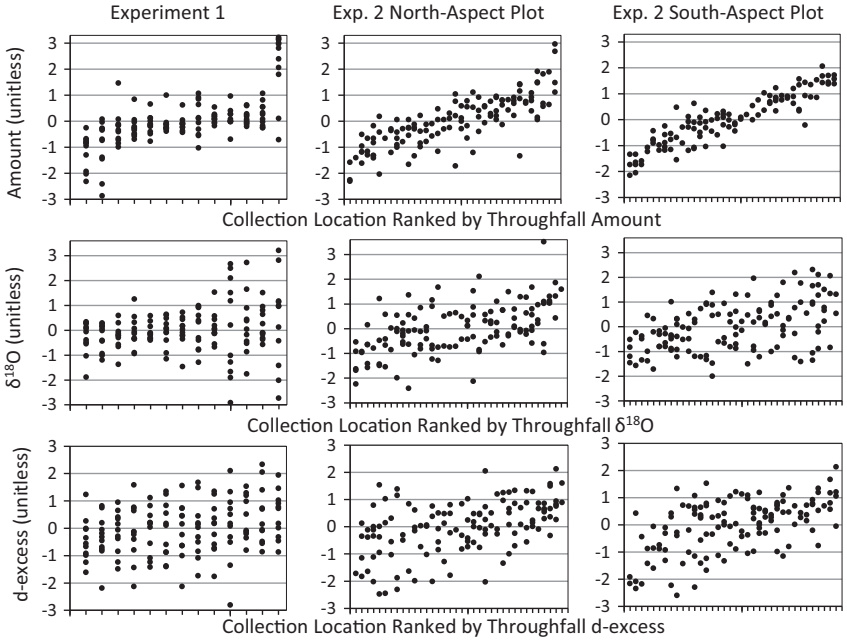

Fig. 2. Time-stability plots. Data plotted were normalized amount, $\delta^{18}O$, and d-excess of throughfall for Experiment 1, Experiment 2 south-aspect-plot, and Experiment 2 north-aspect-plot. Each point refers to a single measurement event at a single location, with the values normalized $\tilde{x} = \frac{x_i - \bar{x}}{\sigma}$. Collectors were ranked by the mean of the dependent variable.

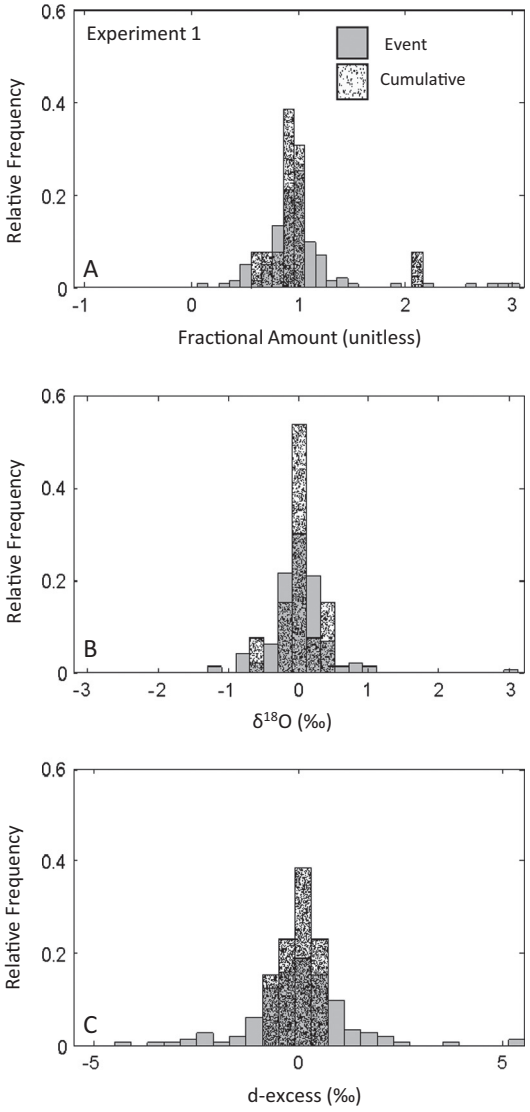

Fig. 3. Histograms of observations from Experiment 1 showing event samples (individual) or cumulative mean samples (cumulative) for (A) fractional amount (collector amount/mean amount), (B) $\delta^{18}O$ deviation from the event or cumulative mean, and (C) d-excess deviation from the cumulative or event mean.

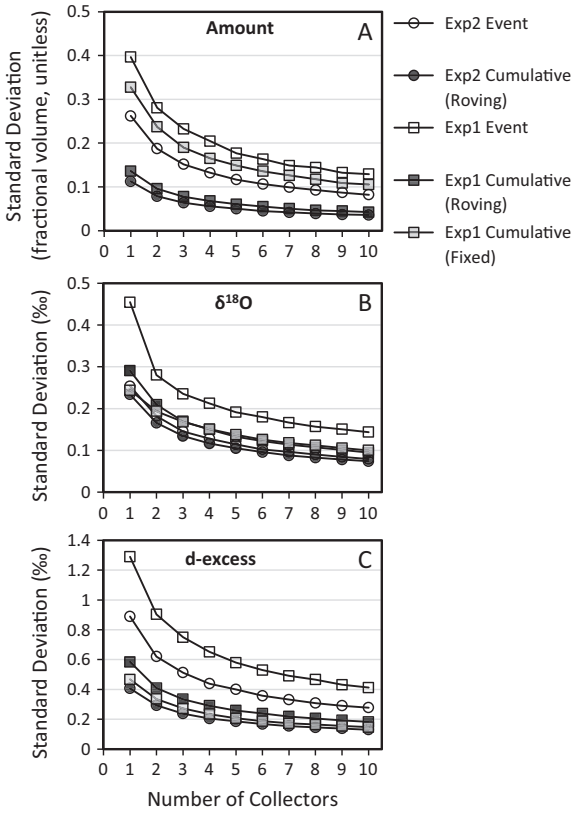

Fig. 4. Simulated effects of sample size and sampling strategy on throughfall measurement deviation from the true mean for cumulative (using fixed position collectors or roving collectors) and individual event sampling of throughfall amount (A), $\delta^{18}O$ (B), and d-excess (C).

Table 2
Pearson correlation coefficients between distance from nearest tree stem and throughfall amount, $\delta^{18}O$, and d-excess in Experiment 2.

Collection Period	South Aspect Plot			North Aspect Plot		
	Amount	$\delta^{18}O$	d-excess	Amount	$\delta^{18}O$	d-excess
2.1	0.49**	0.06	0.04	0.33	0.19	−0.03
2.2	0.66***	−0.28	−0.03	0.14	−0.23	−0.02
2.3	0.35	0.15	−0.48**	0.33	0.36	−0.23
2.4	0.16	0.09	0.25	−0.02	−0.26	−0.05
2.5	0.15	−0.12	−0.04	0.47*	0.11	0.45*
2.6	0.38	0.18	0.19	0.20	−0.27	0.17
2.7	0.45*	−0.04	0.05	0.02	0.43*	−0.11
Cumulative Mean	**0.48****	**−0.09**	**−0.07**	**0.27**	**0.10**	**0.04**

* $p < 0.10$.
** $p < 0.05$.
*** $p < 0.01$.

for individual events and cumulative means (Table 2). Amount was positively correlated with distance for cumulative mean TF amount on the SAP, although only 23% of variability was explained. Some individual events had significant relationships between distance from stem and amount; however these were not consistent in time or between plots (Table 2). The two events with the strongest relationship between location and amount (SAP only) were the highest rainfall sampling periods; isotopic composition did not show the same relationship for these events.

Amount was weakly spatially autocorrelated, in that variance of TF amount increased with lag to a correlation length of approximately 3 m; this trend was stronger at the SAP. In contrast, there was no detectable spatial autocorrelation for $\delta^{18}O$ or d-excess.

4. Discussion

4.1. Spatial variability of event and cumulative TF

The spatial variability of TF $\delta^{18}O$ and d-excess was high and not related to TF amount. Others have similarly found high intra-event spatial variation of TF isotopic composition and low correlation with TF amount. Kato et al. (2013) observed ranges for $\delta^{18}O$ that exceeded 1‰ for individual events. Brodersen et al. (2000) reported spatial ranges of up to 3‰ for $\delta^{18}O$ for samples collected weekly (even with averaging isotopic composition over up to three collectors). This high spatial variation has been hypothesized to be a function of heterogeneity in storage capacities and flow-paths within the canopy (Allen et al., 2014; Brodersen et al., 2000; Kato et al., 2013). However, the lack of correlation between amount and isotopic composition suggests multiple processes controlling variability.

We found event-mean TF was generally heavier in ^{18}O compared to rainfall, consistent with others (Brodersen et al., 2000; DeWalle and Swistock, 1994; Ikawa et al., 2011; Kato et al., 2013; Liu et al., 2008; Saxena, 1986). Nevertheless, the difference between TF and P_g ^{18}O was not related to event size or proportional

to interception loss. Spatially varying evaporative fractionation seems an unlikely cause for large spatial variations in TF isotopic composition because any isotopic exchange with intra-canopy vapor would mitigate spatial variations in evaporative fractionation (Kendall, 1993). However, fine details of exchange and evaporative processes cannot be resolved with the present data. In Exp1, ^{18}O in TF was not consistently heavier than ^{18}O in P_g, suggesting a complex interaction of mixing, exchange, and evaporation. However, in Exp2, which had higher interception loss and lower humidity, d-excess was related to event size and interception loss, indicating that evaporation could contribute to resultant isotopic composition. During both Exp1 and Exp2, Δd-excess was not always positive, which cannot be achieved by evaporation alone (Dansgaard, 1964) so mixing and exchange processes also must have occurred.

Complexity in isotopic signal suggests a complex suite of processes within the canopy. Because numerous canopy processes affect isotopic composition, it is unreasonable to expect simple relationships; this is supported by the results of multiple previous studies (Brodersen et al., 2000; DeWalle and Swistock, 1994; Ikawa et al., 2011; Kato et al., 2013; Liu et al., 2008). However, even without such expectations, this study yielded a surprising lack of interrelationships between the rainfall amount and intensity and the spatial variation in d-excess and $\delta^{18}O$. The effects of evaporation, isotopic exchange, and residual water (Allen et al., 2014) should all have greater effects in smaller storms with lower intensity.

It has been observed elsewhere that storm-total TF is isotopically heavier than P_g and that this is a function of 'selection' (DeWalle and Swistock, 1994; Gat and Tzur, 1968). That is, the variable transmission of precipitation with temporally varying isotopic composition. The justification is that storms often become isotopically lighter throughout the event due to the rainout effect (Kendall and Caldwell, 1998); this results in the last rain increment, the lightest, remaining on the canopy after the storm and not contributing to the net TF isotopic composition (Brodersen et al., 2000; DeWalle and Swistock, 1994; Gat and Tzur, 1968). However, this simple model cannot explain all variability because precipitation does not always become isotopically lighter throughout an event (Coplen et al., 2008).

Selection would affect spatial variability because TF is the output from the spatiotemporally varying mixture of canopy components involved in the interception process, such as the splash from foliage and branches (Dunkerley, 2009), drip points from bark (Herwitz, 1987), or foliar storage overflow. All of these components have different residence times (Levia et al., 2011) and thus different isotopic compositions, despite relatively small storage capacities, because the isotopic composition of precipitation can change rapidly (Coplen et al., 2008; Pangle et al., 2013). As these pools contribute to varying flowpaths within and from the canopy, the output would have a spatially and temporally varying isotopic composition.

4.2. Temporal stability and heterogeneity of accumulated seasonal throughfall

For both experiments, the spatial pattern of TF amount was mostly stable (Fig. 2), consistent with other studies (Gerrits et al., 2010; Keim et al., 2005; Raat et al., 2002; Staelens et al., 2006; Whelan and Anderson, 1996). We observed both patch stability (Exp1) and general stability (Exp2 at the SAP) for TF amount; Exp2 NAP had elements of both for TF amount. Patch stability without general stability would suggest there are stable locations that have different controls over TF generation than at unstable locations (Allen et al., 2014); this could be a tool in distinguishing locations with TF generated from different within canopy processes, such as drip points (stable) versus splash droplets (Dunkerley, 2009). General stability suggests that there is a more continuous range in variation which we speculate may be related to variation in local canopy storage. However, the differences in trends between Exp1 and Exp2 time-stability plots could also have resulted from the greater number of collectors and fewer number of events in Exp2.

Relative isotopic composition was generally not temporally stable. One potential cause of the lack of temporal stability in isotopic composition is that the canopy retains pre-event moisture (Allen et al., 2014). Another possibility would be varying times in activation of flow paths associated with a complex selection effect. Although time-stability plots are indicative of such a process, further insights may require sampling with greater temporal resolution or directly sampling pools within the canopy to better understand TF generation and the mixing processes within the canopy.

For cumulative TF, the decrease in variation from event sampling for TF isotopic composition exceeded that of amount because of these differences in stability. The inter-event variation without persistent locations of heavy or light isotopes is an important finding regarding sampling the soil–water end member because it suggests reduced spatial variation in the soil.

4.3. Spatial controls over TF variability

The stability of TF amount suggests that there are deterministic controls over spatial variability, likely related to canopy architecture (Staelens et al., 2006). Our observed correlation length scale of around 3 m is consistent with studies that found canopy measurements related to amount variation (Gerrits et al., 2010; Staelens et al., 2006). Keim et al. (2005) observed similar correlation lengths but did not observe correlation between amount and position with respect to stem. Isotopic composition was not autocorrelated at the scale we measured or related to collector distance from stem. Even though TF amount was significantly related to distance from stem on average, this was driven by a few specific events. Distance from stem may have been only weakly correlated with TF parameters because distance from stem is not necessarily the most appropriate index of canopy structure. Others have found better relationships between TF measurements and alternate indices such as canopy cover (Staelens et al., 2006) or LAI (Fleischbein et al., 2005).

The first two events of Exp2, which were the largest events, had the strongest relationship between TF and distance from stem. The relationship between distance from stem and relative amount was stronger for larger storms, which conflicts with previous findings of weaker spatial patterns with large storms (Bouten et al., 1992; Keim et al., 2005; Marin et al., 2000). Although weekly precipitation was large in Exp2, individual events contributing to each sampling period generally were small and possibly insufficient for developing persistent drip points (Herwitz, 1987).

The differences between the NAP and SAP (Exp2) were apparent in the TF amounts. Interception loss was higher, temporal stability of patterns was stronger, the variogram had a more distinct trend, and the relationship with distance from stem was more significant in the SAP than the NAP. Although not quantified, we hypothesize this may have been due to aspect effects on crown forms; trees on the SAP generally had a more conical crown form with gaps whereas the NAP crowns were overlapped resulting in a canopy with more even thickness.

The known controls over TF isotopic variation—selective storage (Brodersen et al., 2000; Ikawa et al., 2011), isotopic fractionation (Ikawa et al., 2011; Kato et al., 2013; Kendall, 1993; Liu et al., 2008), or pre-event moisture (Allen et al., 2014; Gat and Tzur, 1968)—could make TF either isotopically lighter or heavier than P_g depending on the ambient vapor and temporal variation of P_g. TF amount can similarly have differential responses to variations in canopy storage; for example, Veneklaas and Van Ek (1990) found

certain locations were drip points in some events but yielded lower amounts due to high canopy storage in other events. For these reasons it is not surprising that patterns of collector-mean TF isotopic compositions were weak and not related to distances from stem.

In contrast with our results, we expected $\delta^{18}O$ and d-excess of individual periods would correlate with distance from stem, with a positive correlation or negative correlation depending on storm characteristics. Brodersen et al. (2000) found different TF amounts and isotopic compositions between inner and peripheral canopy space. Differences in canopy thickness and storage would also affect the selection processes (Saxena, 1986) or amount of pre-event canopy moisture (Allen et al., 2014). Similarly, Kato et al. (2013) found that amount was related to distance from stem but isotopic composition was not. We hypothesize that the lack of well-defined spatial controls over isotopic composition arose from sampling intervals that were composed of multiple events, obscuring expected spatial relationships for individual events.

4.4. Implications for TF sampling

Spatial variability of TF isotopic composition must be considered when sampling throughfall as an end member for isotope applications. We have demonstrated that single collector samples can potentially result in errors exceeding 3‰ $\delta^{18}O$. While the sampling simulations suggest errors are more likely <0.9‰ (±2SD) with a single collector, depending on application, this could be a large concern. Kubota and Tsuboyama (2003) showed the TF − P_g differences (generally smaller than our observed variability within TF), could result in errors in separating source contributions to streamflow. Because the isotopic difference between mean TF and P_g can vary substantially in magnitude and direction (Table 1), a correction factor for estimating TF isotopic composition from P_g is not ideal. Thus we recommend use of multiple TF collectors and reporting variation among samples.

For sampling TF amount, roving collectors reduced variability of sample means because the amount pattern was stable. In contrast, the lack of temporal stability in isotopic composition negates the need for roving samplers. Therefore, common strategies for sampling TF amount involving roving or randomly relocating collectors (e.g., Holwerda et al., 2006) may be unnecessary for reducing isotopic uncertainty. The lack of temporal stability in isotopic composition means that fewer collectors are required in cumulative sampling than if there was stability.

The reduced and more consistent spatial variability in Exp2 compared to Exp1 (Fig. 1) indicates that more collectors, longer collection times, and larger collectors smoothed variability. Accordingly, the sampling simulation showed that with Exp2, fewer collectors were required for standard deviations equivalent with Exp1 (Fig. 4). Although not specifically tested in this study, the lack of spatial autocorrelation in isotopic composition makes using larger collectors a reasonable solution, although it would be less appropriate for amount sampling. Longer time periods are not always possible because of study requirements and fractionation of the collected sample becomes more likely unless specifically prevented (Mook and De Vries, 2001).

Designing sampling strategies for TF isotopic composition remains difficult because few studies have been conducted to understand the sources of variability. This study focused on TF isotopic composition in a small area (scale of meters to tens of meters) with a relatively homogeneous canopy. Additional sources of variability at larger scales include variations in forest type (Brodersen et al., 2000; DeWalle and Swistock, 1994) and the effects of topography on rainfall isotopic variability prior to interception (Ingraham, 1998; McGuire et al., 2005).

5. Conclusions

This study showed large spatial variations of isotopic composition for throughfall of both individual events and season totals that do not correspond with throughfall amount. Among collectors located meters to tens of meters apart, the range of $\delta^{18}O$ spatial variability generally exceeded 1‰, was as high as 3.7‰ (Exp1) and 1.9‰ (Exp2) for individual events, and was 1.0‰ for season-total (Exp1). Overall, no general controls over the spatial pattern could be inferred. Stable spatial patterns of TF depth were observed but stable patterns of isotopic composition were not. The accumulation of non-persistent spatial patterns of isotopic composition resulted in reduced spatial variability of cumulative seasonal TF. Accordingly, roving samplers reduced variability in cumulative amount sampling but not in isotope sampling. Studies characterizing throughfall as an end member should report the variability among multiple collectors rather than means alone, regardless of spatial extent. Ultimately, the ideal number of collectors or size of collectors is dependent on the level of confidence required and the magnitude of variability observed.

Acknowledgements

Data, facilities, and financial support were provided by HJ Andrews Experimental Forest, funded by the National Science Foundation's Long-Term Ecological Research Program (DEB 08-23380), US Forest Service Pacific Northwest Research Station, and Oregon State University.

References

Allen, S.T., Brooks, J.R., Keim, R.F., Bond, B.J., McDonnell, J.J., 2014. The role of pre-event canopy storage in throughfall and stemflow by using isotopic tracers. Ecohydrology 7. http://dx.doi.org/10.1002/eco.1408.

Bond, B.J., Jones, J.A., Moore, G., Phillips, N., Post, D., McDonnell, J.J., 2002. The zone of vegetation influence on baseflow revealed by diel patterns of streamflow and vegetation water use in a headwater basin. Hydrol. Process. 16, 1671–1677. http://dx.doi.org/10.1002/hyp.5022.

Bouten, W., Heimovaara, T.J., Tiktak, A., 1992. Spatial patterns of throughfall and soil water dynamics in a Douglas fir stand. Water Resour. Res. 28, 3227–3233. http://dx.doi.org/10.1029/92WR01764.

Brodersen, C., Pohl, S., Lindenlaub, M., Leibundgut, C., Wilpert, K.v, 2000. Influence of vegetation structure on isotope content of throughfall and soil water. Hydrol. Process. 14, 1439–1448. http://dx.doi.org/10.1002/1099-1085(20000615)14:8<1439::AID-HYP985>3.0.CO;2-3.

Coenders-Gerrits, A.M.J., Hopp, L., Savenije, H.H.G., Pfister, L., 2013. The effect of spatial throughfall patterns on soil moisture patterns at the hillslope scale. Hydrol. Earth Syst. Sci. 17, 1749–1763. http://dx.doi.org/10.5194/hess-17-1749-2013.

Coplen, T.B., Bohlke, J.K., De Bievre, P., Ding, T., Holden, N.E., Hopple, J.A., Krouse, H.R., Lamberty, A., Peiser, H.S., Revesz, K., Rieder, S.E., Rosman, K.J.R., Roth, E., Taylor, P.D.P., Vocke, R.D., Xiao, Y.K., 2002. Isotope-abundance variations of selected elements (IUPAC Technical Report). Pure Appl. Chem. 74, 1987–2017. http://dx.doi.org/10.1351/pac200274101987.

Coplen, T.B., Neiman, P.J., White, A.B., Landwehr, J.M., Ralph, F.M., Dettinger, M.D., 2008. Extreme changes in stable hydrogen isotopes and precipitation characteristics in a landfalling Pacific storm. Geophys. Res. Lett. 35, L21808. http://dx.doi.org/10.1029/2008GL035481.

Dansgaard, W., 1964. Stable isotopes in precipitation. Tellus 16, 436–468. http://dx.doi.org/10.1111/j.2153-3490.1964.tb00181.x.

DeWalle, D.R., Swistock, B.R., 1994. Differences in oxygen-18 content of throughfall and rainfall in hardwood and coniferous forests. Hydrol. Process. 8, 75–82. http://dx.doi.org/10.1002/hyp.3360080106.

Dunkerley, D.L., 2009. Evaporation of impact water droplets in interception processes: historical precedence of the hypothesis and a brief literature overview. J. Hydrol. 376, 599–604. http://dx.doi.org/10.1016/j.jhydrol.2009.08.004.

Fleischbein, K., Wilcke, W., Goller, R., Boy, J., Valarezo, C., Zech, W., Knoblich, K., 2005. Rainfall interception in a lower montane forest in Ecuador: effects of canopy properties. Hydrol. Process. 19, 1355–1371. http://dx.doi.org/10.1002/hyp.5562.

Gat, J.R., 1996. Oxygen and hydrogen isotopes in the hydrologic cycle. Annu. Rev. Earth Planet. Sci. 24, 225–262. http://dx.doi.org/10.1146/annurev.earth.24.1.225.

Gat, J.R., Tzur, Y., 1968. Modification of the isotopic composition of rainwater by processes which occurs before groundwater recharge. In: Isotope Hydrology, Proc. Symp. Vienna 1966, International Atomic Energy Agency, pp. 49–60.

Gerrits, A.M.J., Pfister, L., Savenije, H.H.G., 2010. Spatial and temporal variability of canopy and forest floor interception in a beech forest. Hydrol. Process. 24, 3011–3025. http://dx.doi.org/10.1002/hyp.7712.

Goldsmith, G.R., Muñoz-Villers, L.E., Holwerda, F., McDonnell, J.J., Asbjornsen, H., Dawson, T.E., 2012. Stable isotopes reveal linkages among ecohydrological processes in a seasonally dry tropical montane cloud forest. Ecohydrology 5, 779–790. http://dx.doi.org/10.1002/eco.268.

Halpern, C.B., Dyrness, C., 2010. Plant succession and biomass dynamics following logging and burning in Watersheds 1 and 3, Andrews Experimental Forest, 1962 to Present.

Halpern, C.B., Franklin, J.F., 1990. Physiognomie development of Pseudotsuga forests in relation to initial structure and disturbance intensity. J. Veg. Sci. 1, 475–482. http://dx.doi.org/10.2307/3235781.

Herwitz, S.R., 1987. Raindrop impact and water flow on the vegetative surfaces of trees and the effects on stemflow and throughfall generation. Earth Surf. Process. Landf. 12, 425–432. http://dx.doi.org/10.1002/esp.3290120408.

Holwerda, F., Scatena, F.N., Bruijnzeel, L.A., 2006. Throughfall in a Puerto Rican lower montane rain forest: a comparison of sampling strategies. J. Hydrol. 327, 592–602. http://dx.doi.org/10.1016/j.jhydrol.2005.12.014.

Hopp, L., McDonnell, J.J., 2011. Examining the role of throughfall patterns on subsurface stormflow generation. J. Hydrol. 409, 460–471. http://dx.doi.org/10.1016/j.jhydrol.2011.08.044.

IAEA, 2009. Laser Spectroscopic Analysis of Liquid Water Samples for Stable Hydrogen and Oxygen Isotopes: Performance Testing and Procedures for Installing and Operating the LGR DT-100 Liquid Water Stable Isotope Analyzer. International Atomic Energy Agency, Vienna, Austria.

Ikawa, R., Yamamoto, T., Shimada, J., Shimizu, T., 2011. Temporal variations of isotopic compositions in gross rainfall, throughfall, and stemflow under a Japanese cedar forest during a typhoon event. Hydrol. Res. Lett. 5, 32–36.

Ingraham, N.L., 1998. Isotopic variations in precipitation. In: Kendall, C., McDonnell, J.J. (Eds.), Isotope Tracers in Catchment Hydrology. Elsevier Science, Amsterdam, pp. 87–118.

Kato, H., Onda, Y., Nanko, K., Gomi, T., Yamanaka, T., Kawaguchi, S., 2013. Effect of canopy interception on spatial variability and isotopic composition of throughfall in Japanese cypress plantations. J. Hydrol. 504, 1–11. http://dx.doi.org/10.1016/j.jhydrol.2013.09.028.

Keim, R.F., Skaugset, A.E., Weiler, M., 2005. Temporal persistence of spatial patterns in throughfall. J. Hydrol. 314, 263–274. http://dx.doi.org/10.1016/j.jhydrol.2005.03.021.

Kendall, C., 1993. Impact of isotopic heterogeneity in shallow system on stormflow generation. (Ph.D. Dissertation). University of Maryland, College Park, MD.

Kendall, C., Caldwell, E., 1998. Fundamentals of isotope geochemistry. In: Isotope Tracers in Catchment Hydrology (Developments in Water Science). Elsevier Science, pp. 51–86.

Kendall, C., McDonnell, J.J., 1998. Isotope Tracers in Catchment Hydrology. Elsevier Science, Amsterdam, New York.

Klaus, J., McDonnell, J.J., 2013. Hydrograph separation using stable isotopes: review and evaluation. J. Hydrol. 505, 47–64. http://dx.doi.org/10.1016/j.jhydrol.2013.09.006.

Kubota, T., Tsuboyama, Y., 2003. Intra- and inter-storm oxygen-18 and deuterium variations of rain, throughfall, and stemflow, and two-component hydrograph separation in a small forested catchment in Japan. J. For. Res. 8, 179–190. http://dx.doi.org/10.1007/s10310-002-0024-9.

Levia, D.F., Keim, R.F., Carlyle-Moses, D.E., Frost, E.E., 2011. Throughfall and stemflow in wooded ecosystems. In: Levia, D.F., Carlyle-Moses, D., Tanaka, T. (Eds.), Forest Hydrology and Biogeochemistry, Ecological Studies. Springer, Netherlands, pp. 425–443.

Link, T.E., Unsworth, M., Marks, D., 2004. The dynamics of rainfall interception by a seasonal temperate rainforest. Agric. For. Meteorol. 124, 171–191.

Liu, W.J., Liu, W.Y., Li, J.T., Wu, Z.W., Li, H.M., 2008. Isotope variations of throughfall, stemflow and soil water in a tropical rain forest and a rubber plantation in Xishuangbanna, SW China. Hydrol. Res. 39, 437. http://dx.doi.org/10.2166/nh.2008.110.

Loescher, H.W., Powers, J.S., Oberbauer, S.F., 2002. Spatial variation of throughfall volume in an old-growth tropical wet forest, Costa Rica. J. Trop. Ecol. 18, 397–407. http://dx.doi.org/10.1017/S0266467402002274.

Lutz, J.A., Halpern, C.B., 2006. Tree mortality during early forest development: a long-term study of rates, causes and consequences. Ecol. Monogr. 76, 257–275. http://dx.doi.org/10.1890/0012-9615(2006)076[0257:TMDEFD]2.0.CO;2.

Marin, C.T., Bouten, W., Sevink, J., 2000. Gross rainfall and its partitioning into throughfall, stemflow and evaporation of intercepted water in four forest ecosystems in western Amazonia. J. Hydrol. 237, 40–57. http://dx.doi.org/10.1016/S0022-1694(00)00301-2.

McGuire, K.J., McDonnell, J.J., Weiler, M., Kendall, C., McGlynn, B.L., Welker, J.M., Seibert, J., 2005. The role of topography on catchment-scale water residence time. Water Resour. Res. 41, W05002. http://dx.doi.org/10.1029/2004WR003657.

Mook, W.G., De Vries, J., 2001. Environmental Isotopes in the Hydrological Cycle: Principles and Applications. International Atomic Energy Agency, Vienna, Austria.

Pangle, L.A., Klaus, J., Berman, E.S.F., Gupta, M., McDonnell, J.J., 2013. A new multisource and high-frequency approach to measuring δ^2H and $\delta^{18}O$ in hydrological field studies. Water Resour. Res. 49, 7797–7803. http://dx.doi.org/10.1002/2013WR013743.

Raat, K.J., Draaijers, G.P.J., Schaap, M.G., Tietema, A., Verstraten, J.M., 2002. Spatial variability of throughfall water and chemistry and forest floor water content in a Douglas fir forest stand. Hydrol. Earth Syst. Sci. 6, 363–374.

Ritter, A., Regalado, C.M., 2010. Investigating the random relocation of gauges below the canopy by means of numerical experiments. Agric. For. Meteorol. 150, 1102–1114. http://dx.doi.org/10.1016/j.agrformet.2010.04.010.

Ritter, A., Regalado, C.M., 2014. Roving revisited, towards an optimum throughfall sampling design. Hydrol. Process. 28, 123–133. http://dx.doi.org/10.1002/hyp.9561.

Rothacher, J., 1963. Net precipitation under a Douglas-fir forest. For. Sci. 9, 423–429.

Rothacher, J., 1965. Streamflow from small watersheds on the western slope of the Cascade Range of Oregon. Water Resour. Res. 1, 125–134. http://dx.doi.org/10.1029/WR001i001p00125.

Saxena, R.K., 1986. Estimation of canopy reservoir capacity and Oxygen-18 fractionation in throughfall in a pine forest. In: Nordic Hydrology. Presented at the Nordic Hydrological Conference, Reykjavik (Iceland), August 1986.

Staelens, J., De Schrijver, A., Verheyen, K., Verhoest, N.E.C., 2006. Spatial variability and temporal stability of throughfall water under a dominant beech (*Fagus sylvatica* L.) tree in relationship to canopy cover. J. Hydrol. 330, 651–662. http://dx.doi.org/10.1016/j.jhydrol.2006.04.032.

Tetzlaff, D., Soulsby, C., Hrachowitz, M., Speed, M., 2011. Relative influence of upland and lowland headwaters on the isotope hydrology and transit times of larger catchments. J. Hydrol. 400, 438–447. http://dx.doi.org/10.1016/j.jhydrol.2011.01.053.

Vachaud, G., Passerat De Silans, A., Balabanis, P., Vauclin, M., 1985. Temporal stability of spatially measured soil water probability density function. Soil Sci. Soc. Am. J. 49, 822. http://dx.doi.org/10.2136/sssaj1985.03615995004900040006x.

Veneklaas, E.J., Van Ek, R., 1990. Rainfall interception in two tropical montane rain forests, Colombia. Hydrol. Process. 4, 311–326. http://dx.doi.org/10.1002/hyp.3360040403.

Whelan, M.J., Anderson, J.M., 1996. Modelling spatial patterns of throughfall and interception loss in a Norway spruce (Picea abies) plantation at the plot scale. J. Hydrol. 186, 335–354. http://dx.doi.org/10.1016/S0022-1694(96)03020-X.

Zimmermann, B., Zimmermann, A., Lark, R.M., Elsenbeer, H., 2010. Sampling procedures for throughfall monitoring: a simulation study. Water Resour. Res. 46. http://dx.doi.org/10.1029/2009WR007776.